

# The phase diagram of the quasibinary system $\text{Hg}_3\text{Se}_3/\text{Ga}_2\text{Se}_3$

Martina Kerkhoff, Volkmar Leute\*

*Institut für Physikalische Chemie der Universität Münster, Corrensstrasse 36, Münster 48149, Germany*

Received 2 April 2004; accepted 26 April 2004

## Abstract

The quasibinary system  $\text{Hg}_3\text{Se}_3/\text{Ga}_2\text{Se}_3$  was investigated by X-ray phase analysis and by DTA. The system forms extended regions of solid solutions with zincblende structure. Moreover, it shows at several distinct stoichiometries the formation of superstructures. The phase diagram of this system can be modeled by a Gibbs energy function for a sub-regular system including ordering terms. The thermodynamic factor for interdiffusion was calculated from the excess Gibbs energy function.

© 2004 Elsevier B.V. All rights reserved.

*Materials:*  $\text{Ga}_2\text{Se}_3$ ;  $\text{Hg}_5\text{Ga}_2\text{Se}_8$ ;  $\text{HgGa}_2\text{Se}_4$

*Keywords:* Quasibinary systems; Thermodynamics; Thermodynamic factor; Super structures; Ordering phenomena; Lattice constants; Solid solutions; Chalcogenides; Structural vacancies

## 1. Introduction

Quasibinary alloys of II/VI and III/VI compounds are interesting systems for materials as they yield both extended solid solutions and ordered structures with a high variability of properties. To prepare thermodynamically stable substances the phase diagram of the respective system including miscibility gaps and ordered regions should be known.

For the calculation of the phase diagram of such a quasibinary system the mean molar Gibbs energy as function of temperature and composition is needed. For this purpose both the excess Gibbs energy, normally described by so-called interaction parameters and the Gibbs energies for the transformation between all contributing phases should be known.

Alloys of II/VI and III/VI compounds generally crystallize with the zinc-blende lattice, but because of the stoichiometry of the III/VI compound  $\text{Ga}_2\text{VSe}_3$  the cation sublattice contains structural vacancies  $\text{V}$  in a concentration that is always half that of Ga. These so-called structural vacancies enable ordering processes of the constituents of the cation sublattice leading near special stoichiometric compo-

sitions to the formation of super structures of the zincblende lattice. If the degree of order of such an ordered structure would decrease continuously with increasing distance from its stoichiometric composition until the order has vanished, the Gibbs energy curve of such an ordered phase should approach the Gibbs energy curve of the disordered solid solution at some distance from the stoichiometric composition. Therefore, from a thermodynamic point of view, the standard chemical potentials of the components of a quasibinary ordered phase showing an extended composition region should be the same as those of the components of the surrounding disordered solid solution. Thus, it is favourable to treat such a quasibinary system including super structures, as one single phase with ordered regions. An heuristic method to fulfill this demand is to describe the ordering contributions to the Gibbs energy near the characteristic stoichiometric compositions by additive Gaussian terms [1,2].

The description of the whole sub-solidus region by one single  $g$ -function including ordering terms often yields regions where  $\partial^2 g / \partial k^2 < 0$ . Such regions are to be interpreted as thermodynamically unstable regions, i.e. regions that lead to the formation of miscibility gaps [3]. Thermodynamically, these miscibility gaps are totally equivalent to so-called spinodal miscibility gaps and do not have to correspond to possible phase boundaries between phases with different symmetry.

\* Corresponding author. Tel.: +49-251-83-23422; fax: +49-251-83-23423.

E-mail address: leutev@uni-muenster.de (V. Leute).

This thermodynamic treatment is well adapted for describing the thermodynamic factor depending on the excess Gibbs energy by a continuous function  $F(g^E)$ . This method allows to compare the behaviour of the thermodynamic factor in ordered regions with that in disordered regions.

## 2. Experiments

### 2.1. Methods of preparation and measurement

The binary compounds HgSe and Ga<sub>2</sub>Se<sub>3</sub> were synthesized from the elements and purified as described in [4,5].

X-ray measurements were used to determine the structures and the lattice constants of the equilibrium phases. For this purpose a set of powder mixtures of different molar ratios of the above mentioned binary compounds were prepared. All samples were annealed in evacuated sealed quartz ampoules until thermodynamic equilibrium was attained. Annealing times depending on the annealing temperature extended up to 25 weeks for the lowest annealing temperature of 600 K. To preserve the high temperature equilibrium compositions and structures the annealed samples were quenched in ice-water.

Some experiments to determine the boundaries of miscibility gaps were done by use of an electron microprobe.

DTA measurements were used to determine the solidus and liquidus lines as well as order disorder transformations in the sub-solidus region. HgTe, Zn and In<sub>2</sub>Te<sub>3</sub> were used as standard substances for the temperature calibration. The heating and cooling procedures were carried out at velocities between 15 and 2 K/min. The transition temperature was taken as the limiting value of such series obtained by extrapolation to zero velocity.

### 2.2. X-ray diffraction

#### 2.2.1. General features of the phase diagram

The phase diagram in the sub-solidus region was investigated within the temperature region  $600 \text{ K} \leq T \leq 1100 \text{ K}$ . For all samples that were investigated by X-ray measurements Fig. 1 shows the annealing temperatures, the initial compositions of the samples before annealing and the structures of the equilibrated samples. The meaning of the symbols are given in the legend of the figure. A superposition of two symbols at one site indicates that the corresponding samples are two-phase samples showing the line sets of both phases. By X-ray diffraction three types of superstructures at definite stoichiometries  $k^*$  could be detected:

- At  $k \approx 0.35$  and  $T = 600 \text{ K}$  a tetragonal phase (t1) was detected that corresponds in its X-ray pattern (Fig. 2) totally to the so-called ‘3/8-structure’ that also was observed in other Hg-chalcogenide containing systems. But in all these systems the stoichiometry of the totally ordered structure always was at  $k^* = 3/8 = 0.375$ . Only this composition allows a fully ordered superstructure with a

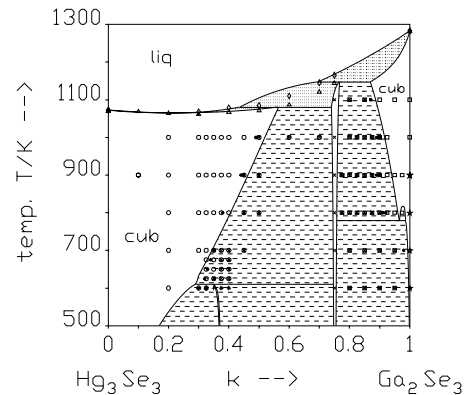


Fig. 1. The phase diagram of the quasibinary system  $(\text{Hg}_{3(1-k)}\text{Ga}_{2k}\text{V})\text{Se}_3$ . (○) cubic (c1), (◻) cubic (c3), (+) tetragonal (t1), (×) tetragonal (t2), (☆) monoclinic (mo), (Δ) DTA signal from heating cycle, (◇) DTA signal from cooling cycle. (●) miscibility limit calculated from lattice constants (Tables 3 and 4), (■) miscibility limit from microprobe measurements.

relatively small unit cell [6]. Thus, we assume that also in the present case the exact stoichiometry is  $k^* = 3/8$ .

- At  $k^* = 0.75$  in the whole investigated temperature region a tetragonal phase (t2) with the chalcopyrite structure,  $\text{HgGa}_2\text{VSe}_4$ , occurs.

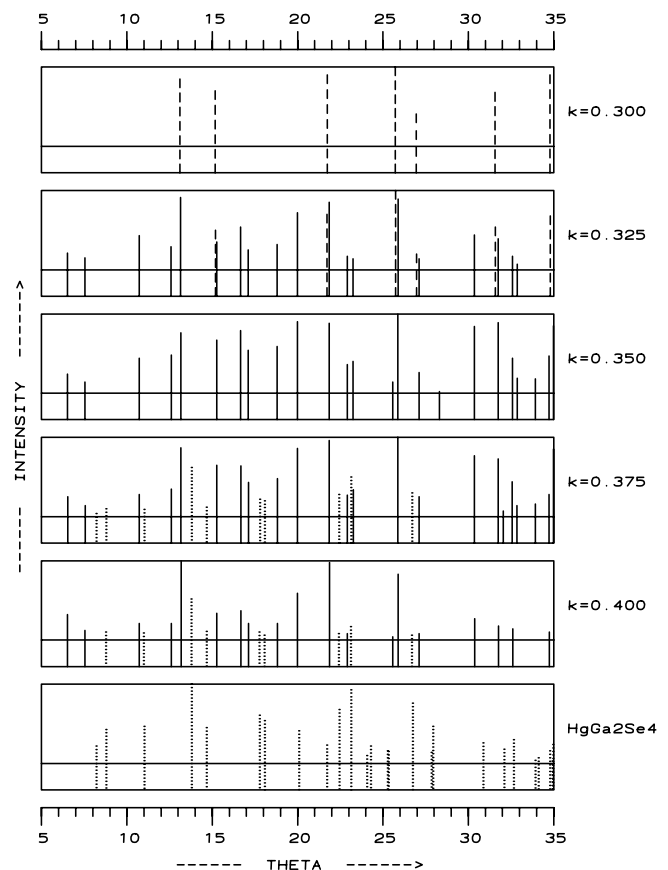


Fig. 2. X-ray patterns of samples annealed at 600 K and quenched to room temperature. The horizontal lines indicate the zero level of X-ray intensity. Dashed lines: ‘zincblende’ reflections (c1), dotted lines: ‘chalcopyrite’ reflections (t2), solid lines: reflections of the tetragonal ‘3/8’-phase (t1).

- At  $k^* = 1.0$  for  $T < 1003$  K the ordered monoclinic  $\beta$  modification of  $\text{Ga}_2\text{VSe}_3$  (mo) exists.

The existence of these three ordered regions causes the occurrence of several miscibility gaps:

- One gap at  $T > \approx 620$  K between the chalcopyrite phase, ( $k \approx 0.75$ ), and the HgSe-rich cubic phase (cl) and an second one between the chalcopyrite phase and the  $\text{Ga}_2\text{Se}_3$ -rich cubic phase (c3).
- At 600 K two additional miscibility gaps could be detected between the tetragonal ‘3/8-phase’ (t1) and either the HgSe-rich cubic phase (c1) or the chalcopyrite phase (t2).
- On the  $\text{Ga}_2\text{Se}_3$ -rich side no miscibility gap could be detected between the cubic solid solution (c3) with the structure of  $\alpha\text{-Ga}_2\text{Se}_3$  and the monoclinic  $\beta\text{-Ga}_2\text{Se}_3$  ( $T < 1000$  K).

### 2.2.2. The so-called 3/8-phase with $k^* = 0.375$

The samples with  $k = 0.325, 0.350, 0.375$  or  $0.400$  that were annealed at 600 K show X-ray patterns (Fig. 2) containing a set of reflections that can be indexed according to the body-centered tetragonal 3/8-structure known from other Hg–chalcogenide containing systems like  $(\text{Hg}_{3-3k}\text{In}_{2k}\text{V}_k)\text{Se}_3$  [6],  $(\text{Hg}_{3-3k}\text{In}_{2k}\text{V}_k)\text{Te}_3$  [7] and  $(\text{Hg}_{3-3k}\text{Ga}_{2k}\text{V}_k)\text{Te}_3$  [8]. In all these systems the stoichiometry of the fully ordered structure corresponds exactly to  $k^* = 0.375$ . Like these known compounds the compound  $\text{Hg}_5\text{Ga}_2\text{VSe}_8$  also crystallizes in space group  $\bar{I}4m2$ , No. 119, the site positions correspond to those given for  $\text{Hg}_5\text{In}_2\text{VTe}_8$  in [9] and the lattice parameters of the homogeneous one-phase sample are:  $a^{\text{t1}} = 828.0$  pm and  $c^{\text{t1}} = 1170.9$  pm (Table 1). This superstructure is correlated to the basic zincblende lattice by  $a^{\text{t1}} = \sqrt{2}a_{\text{zb}}$  and  $c^{\text{t1}} = 2a_{\text{zb}}$ . The tetragonal lattice of  $\text{Hg}_5\text{Ga}_2\text{VSe}_8$  is undistorted, i.e. the experimentally determined lattice constants fulfill the ideal ratio  $c^{\text{t1}}/a^{\text{t1}} = \sqrt{2}$  (Table 1).

For  $k = 0.325$  the set of reflections of this structure is superposed by a line set of the cubic solid solution (cl) and for  $k = 0.375$  and  $0.400$  by the tetragonal line set of the chalcopyrite structure. Only for  $k = 0.350$  the samples show

Table 1

Lattice constants  $a^{\text{t1}}$  and  $c^{\text{t1}}$  calculated from c1–t1 and t1–t2 two-phase samples that were annealed at 600 K;  $k_0$  are the overall compositions of the two-phase samples

	$k_0$			
	0.325	0.350	0.375	0.400
$a^{\text{t1}}$ (pm)	827.9	828.0	826.9	826.2
$c^{\text{t1}}$ (pm)	1170.4	1170.9	1169.1	1168.4
$a_0^{\text{t1}}$ (pm)	585.4	585.5	584.6	584.2
$V_{\text{cell}}$ (nm) <sup>3</sup>	0.802	0.803	0.799	0.798
$k_{\text{t1}}$	0.350	0.348	0.362	0.368
$(c^{\text{t1}}/a^{\text{t1}})^2$	1.999	2.000	1.999	2.000

$a_0^{\text{t1}}$  is the pseudo cubic lattice constant,  $V_{\text{cell}}$  the cell volume,  $k_{\text{t1}}$  are the boundary mole fractions for t1 as calculated from  $a_0^{\text{t1}}$  with Eq. (2).

Table 2

Lattice constants of stoichiometric  $\text{HgGa}_2\text{VSe}_4$  (t2) for different annealing temperatures

	$T$ (K)				
	1000	900	800	700	600
$a$ (pm)	571.3	571.0	571.0	571.6	571.7
$c$ (pm)	1083.1	1082.7	1082.2	1080.9	1080.4
$c/a$	1.896	1.896	1.895	1.891	1.890
$v_{\text{cell}}$ (nm) <sup>3</sup>	0.354	0.353	0.353	0.353	0.353

the pure line set of the 3/8-structure (Fig. 2). This means that this homogeneous sample is non-stoichiometric, i.e. 1/15 of the structural vacancies of the ideal superstructure are occupied by additional Hg ions.

From the Vegard Eq. (2) and from the values of the pseudo cubic lattice constant  $a_0^{\text{t1}}$  (Table 1), the existence region of this ordered ‘3/8-phase’ at 600 K was determined as  $0.35 < k^{\text{t1}} < 0.365$ .

### 2.2.3. The chalcopyrite phase at $k^* = 0.75$

The values for the lattice constants, shown in Table 2 for the stoichiometric chalcopyrite phase at  $k^* = 0.75$ , are derived from measurements on samples quenched from the given annealing temperatures to room temperature. They deviate only little from those reported by Gastaldi et al. [10],  $a = 569.3$  pm,  $c = 1082.6$  pm. The lattice constants  $a$  and  $c$  change only very slightly in dependence on the annealing temperature. Nevertheless, the detected increase of  $c$  between 600 and 1000 K seems to be outside the limit of error.

From the fact that strictly stoichiometric samples quenched from different annealing temperatures yield somewhat different lattice constants, we conclude that the temperature dependent degree of order can be quenched. This is possible, if the activation energy for diffusion in the cation sublattice is rather high.

Table 2 shows that the  $c/a$  ratio slightly increases with increasing annealing temperatures, but even at 1000 K it still deviates rather strongly from the ideal value of 2. According to Gastaldi et al. [10] a value of  $c/a = 2$  would be characteristic for only partially ordered structures, as for example for  $\beta\text{-(HgGa}_2\text{V)}\text{Te}_4$ , in which the Hg ions are well ordered, whereas the trivalent Ga ions and the structural vacancies are randomly disordered on the remaining sites in the cation sublattice. Obviously, in the telluride lattice, due to its higher lattice constants, the activation enthalpy for the Ga-diffusion is decreased so distinctly that there the ordering of the Ga ions is thermally disturbed. However, a  $c/a$ -value distinctly lower than 2 indicates a structure, where not only the big Hg ions, but additionally the smaller Ga ions are ordered. Thus, the fact that for  $(\text{HgGa}_2\text{V)}\text{Se}_4$ -even at high temperatures-the ratio  $c/a$  (Table 2) deviates rather much from the ideal value and decreases only very slightly with decreasing annealing temperature shows that nearly the full degree of order is probably already reached at 1000 K.

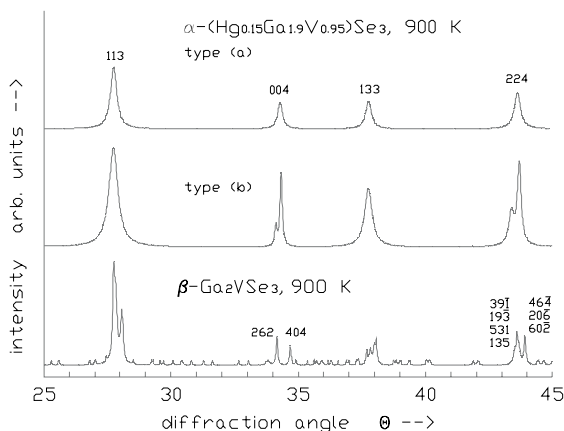


Fig. 3. Sections of the X-ray patterns of: (a) cubic  $\alpha$ - $\text{Ga}_2\text{VSe}_3$  (c3, type a); (b) a modified  $\alpha$ - $\text{Ga}_2\text{VSe}_3$  with split  $(h+k+l) = 2n$  reflections (c3, type b); (c) fully ordered  $\beta$ - $\text{Ga}_2\text{VSe}_3$  (mo).

#### 2.2.4. The monoclinic $\beta$ - $\text{Ga}_2\text{VSe}_3$ at $k^* = 1$

In [11] it was reported that beside the cubic modification, called  $\alpha$ - $\text{Ga}_2\text{VSe}_3$  (Fig. 3, type (a)), an ordered  $\beta$ -modification of  $\text{Ga}_2\text{VSe}_3$  exists [5]. The X-ray pattern of this phase shows more than 100 sharp reflections (Fig. 3).

Experiments showed that by an annealing of 122 days at 800 K pure  $\alpha$ - $\text{Ga}_2\text{VSe}_3$  can be transformed totally to the ordered  $\beta$ -modification. This ordered modification being stable below 1003 K [12] shows only a very restricted solubility for HgSe. Adding 2.5 mol% of  $\text{Hg}_3\text{Se}_3$  to  $\text{Ga}_2\text{VSe}_3$  yields after the same annealing procedure at 800 K an  $\alpha$ - $\text{Ga}_2\text{VSe}_3$  pattern together with only the most intensive superstructure reflections of the  $\beta$ - $\text{Ga}_2\text{VSe}_3$  plus some very weak and diffuse reflections at positions, where in the  $\beta$ -modification groups of reflections occur. In samples with  $k \leq 0.95$  only the reflections of  $\alpha$ - $\text{Ga}_2\text{VSe}_3$  still occur.

After annealing at 900 or 1000 K the patterns of all  $\text{Ga}_2\text{Se}_3$  rich alloys have changed—compared to the pattern of  $\alpha$ - $\text{Ga}_2\text{VSe}_3$ —in so far as those reflections fulfilling the condition  $(h+k+l) = 2n$  have split into doublets (Fig. 3, type (b)). Moreover, all superstructure reflections of the  $\beta$ - $\text{Ga}_2\text{VSe}_3$  have vanished totally. However, a comparison of such X-ray diagrams with that of monoclinic  $\beta$ - $\text{Ga}_2\text{VSe}_3$  shows interesting similarities: for example the pair arising near the cubic 224 position corresponds to the two groups  $(39\bar{1}, 19\bar{3}, 531, 135)$  and  $(464, 602, 206)$  of the monoclinic  $\beta$ - $\text{Ga}_2\text{VSe}_3$ . This indicates that there is still an ordering tendency in the solid solutions, but the degree of order must have strongly decreased.

At  $T = 600$  and  $700$  K the X-ray patterns of samples with  $0.75 < k \leq 0.95$  consist of the superposition of the line sets of the  $\alpha$ - $\text{Ga}_2\text{VSe}_3$  and of the chalcopyrite structure. For  $k \geq 0.95$ , where the predominant part of these two-phase samples consists of nearly pure  $\text{Ga}_2\text{VSe}_3$ , some of the most intensive superstructure reflections of the monoclinic structure are additionally to be seen. Thus, at temperatures below 800 K the miscibility gap extends between nearly stoichiometric phases of tetragonal  $\text{HgGa}_2\text{VSe}_4$  (t2) and monoclinic

$\beta$ - $\text{Ga}_2\text{VSe}_3$  (mo). At higher temperatures the two-phase samples consist of the chalcopyrite phase (t2) and the cubic  $\alpha$ - $\text{Ga}_2\text{VSe}_3$  (c3). Obviously, the occupation of only a few % of the structural vacancies by Hg atoms disturbs distinctly the ordering of the Ga atoms in the metal sublattice. But experimentally, a phase boundary between the ordered monoclinic  $\beta$ - $\text{Ga}_2\text{VSe}_3$  and a solid solution with the cubic  $\alpha$ - $\text{Ga}_2\text{VSe}_3$  structure could never be detected. As already mentioned above, we assume that the observed X-ray patterns of the so-called  $\alpha$ - $\text{Ga}_2\text{VSe}_3$  correspond to a partially ordered structure of  $\text{Ga}_2\text{VSe}_3$  and the extension of locally ordered regions becomes smaller and smaller with increasing Hg content in such a way that the intensity of the superstructure reflections vanish without any perceptible discontinuity.

#### 2.2.5. Lattice constants of the solid solutions

As in nearly all quasibinary II/VI–III/VI-systems the pure II/VI-component HgSe crystallizes in the zincblende lattice and the pure III/VI-component  $\text{Ga}_2\text{VSe}_3$  as well as the solid solutions of the two components in the so-called defect zincblende lattice, where the constituents Hg, Ga, and V in the cation sublattice are more or less randomly distributed. The cubic lattice constants measured on homogeneous  $\text{Ga}_2\text{Se}_3$ -rich samples can be described in a rather good approximation by a function depending linearly on the  $\text{Ga}_2\text{Se}_3$  mole fraction  $k$ . With  $a(\text{HgSe}) = 608.6$  pm and  $a(\text{Ga}_2\text{Se}_3) = 545.1$  pm this ‘Vegard’ function reads (Fig. 4):

$$a(k)/\text{pm} = 608.6 - 63.5k, \quad \text{valid for } k > 0.6 \quad (1)$$

The homogeneous HgSe-rich samples, equilibrated at 1000 K, extend from the pure HgSe ( $k = 0$ ) up to a mole fraction of at least  $k = 0.5$  (Fig. 4). But their lattice constants belong to a somewhat steeper line described by Eq. (2)

$$a(k)/\text{pm} = 608.6 - 66.0k, \quad \text{valid for } k < 0.6 \quad (2)$$

As the ordered structures  $\text{Hg}_5\text{Ga}_2\text{VSe}_8$  (t1)  $\text{HgGa}_2\text{VSe}_4$  (t2) are superstructures of the zincblende lattice, the linear functions Eqs. (1) and (2) can be applied also on these superstructures if so-called pseudo cubic lattice constants  $a_0^\Phi$  for the tetragonal superstructures  $\Phi = \text{t1}$  or  $\text{t2}$  are introduced. In the case of the undistorted 3/8-structure this constant is

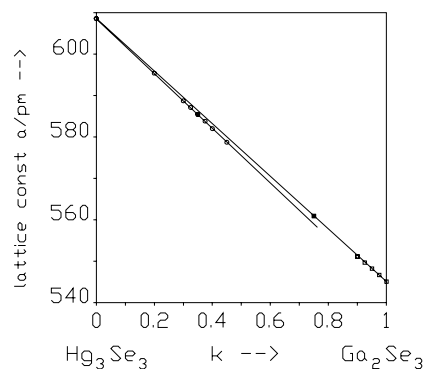


Fig. 4. Linear relationships  $a(k)$  for cubic and pseudo cubic lattice constants: (○) c1, (●) t1, (□) c3, (■) t2 (Eqs. (1) and (2)).

defined as  $a_0^1 = (V_{\text{cell}}/4)^{1/3}$  and in the case of the distorted chalcopyrite structure with  $c/a < 2$ , as  $a_0^2 = (V_{\text{cell}}/2)^{1/3}$ .

One obtains for the pseudo cubic lattice constants from the cell volume  $V_{\text{cell}}^{\text{t2}} = 0.803 \text{ nm}^3$  of the homogeneous ‘3/8-phase’ (Table 1) a value of  $a_0^1 = 585.5 \text{ pm}$ , and from the cell volume  $V_{\text{cell}}^{\text{t2}} = 0.353 \text{ nm}^3$  of the chalcopyrite phase (Table 2) a value of  $a_0^2 = 560.9 \text{ pm}$ . With these lattice constants one obtains from Eq. (2) a mole fraction of  $k^1 = 0.361$  for the ‘3/8-phase’ in rather good accordance with the results from X-ray diffraction, and from Eq. (1) a mole fraction of  $k^2 = 0.751$ . These results show that these equations cannot only be used to describe the lattice constants of the solid solutions, but also those of the adjacent ordered phases (Fig. 4).

### 2.2.6. Limits of miscibility

The lattice constants  $a$  for the HgSe-rich cubic phase (c1) in equilibrium with the chalcopyrite phase (t2) can be determined from the cubic line set of the X-ray patterns of the two-phase samples. Eq. (2) can then be used to calculate the mole fractions  $k^1$  for the cubic boundary of the miscibility gap (Table 3).

For the lattice parameters of the chalcopyrite phase (t2) in equilibrium with the HgSe-rich cubic phase (c1) one obtains from the tetragonal line sets of the two-phase samples nearly constant values with only statistical scattering. The mean values taken from all temperatures and compositions are  $\langle a \rangle = 571.7 \text{ pm}$  and  $\langle c \rangle = 1081.3 \text{ pm}$ . Considering the error limits of measurement these values are nearly the same as those for the strict stoichiometric compound  $\text{HgGa}_2\text{VSe}_4$ :  $\langle a \rangle = 571.2 \text{ pm}$  and  $\langle c \rangle = 1081.8 \text{ pm}$  (Table 2). Thus there is no measurable solubility for HgSe in the chalcopyrite phase  $\text{HgGa}_2\text{VSe}_4$ .

The limit  $k^2$  of the existence region of the chalcopyrite phase (t2) in equilibrium with the solid solution (c3), i.e. the solubility limit of  $\text{Ga}_2\text{VSe}_3$  in  $\text{HgGa}_2\text{VSe}_4$  (Table 4), was determined by using Eq. (1) and the values for the pseudo cubic lattice constant  $a_0^2$  derived from the two-phase samples.

The composition  $k^{c3}$  of the  $\text{Ga}_2\text{VSe}_3$ -rich boundary of the miscibility gap was also determined by using Eq. (1), but in this case the lattice constant  $a^{c3}$  (Table 4) as de-

Table 3  
Miscibility limit of the HgSe-rich cubic phase (c1)

T (K)	$k^1$
1000	0.494
900	0.440
800	0.377
700	0.350
675	0.341
650	0.333
625	0.324
600	0.300

Table 4

Lattice constants calculated from t2–c3 two-phase samples and mole fractions  $k^2$  for the tetragonal and  $k^{c3}$  for the cubic boundaries of the miscibility gap between chalcopyrite (t2) and  $\text{Ga}_2\text{Se}_3$ -rich solid solution (c3)

	T (K)					
	1100	1000	900	800	700	600
$a^{\text{t2}}$ (pm)	567.1	566.4	568.0	569.9	571.2	572.0
$c^{\text{t2}}$ (pm)	1084.1	1084.8	1083.6	1081.9	1080.4	1079.6
$a_0^{\text{t2}}$ (pm)	558.8	558.3	559.3	560.1	560.4	560.9
$k^{\text{t2}}$	0.78	0.79	0.78	0.76	0.76	0.75
$a^{c3}$ (pm)	553.6	551.9	551.9	550.2	546.6	545.6
$k^{c3}$	0.87	0.89	0.89	0.92	0.98	0.99

rived from the cubic line set of the two phase samples—was used.

### 2.3. DTA-measurements

#### 2.3.1. Order–disorder transition

Samples within the composition range  $0.35 \leq k \leq 0.40$  show a small endothermic effect near 630 K in the heating curves and a corresponding effect in the cooling curves. The effect is sharpest at  $k = 0.375$  and can no more be detected for  $k = 0.325$ . This effect is due to an order–disorder transformation near the transition temperature between a tetragonally ordered 3/8-phase and a cubic disordered solid solution with zincblende structure. This effect can be observed, because at these low temperatures the peritectoid decomposition-demanding diffusion processes of the big Hg ions is not fast enough compared to the velocity of the temperature change during a DTA cycle.

#### 2.3.2. Liquidus–solidus

Fig. 1 shows the compositions of the samples and the temperatures of the DTA peaks. The solidus and liquidus curves yield a common minimum at  $k_{\text{az}} = 0.21$ ,  $T_{\text{az}} = 1064 \text{ K}$ . Thus, this system behaves azeotropic. The compound  $\text{HgGa}_2\text{VSe}_4$  (t2) does not melt congruently, but forms a peritectic at  $T \approx 1150 \text{ K}$ . A second peritectic point, where the melt is in equilibrium with a HgSe-rich cubic solid solution and a HgSe-saturated  $\text{HgGa}_2\text{VSe}_4$  (t2), must occur between these two temperatures 1064 and 1150 K.

## 3. Calculation of the phase diagram

### 3.1. General procedures

The mean molar Gibbs energy of a solid solution can be split into three terms: a standard, a mixing and an excess term.

$$g = g^0 + g^M + \left( g^{E,n} + \sum g_{k*}^s \right) \quad (3)$$

To calculate the normal excess term  $g^{E,n}$  we used a model with temperature dependent interaction parameters,  $g^{E,n} = h^E - T s^E$ , where the interaction parameters depend linearly on the mole fraction  $k$ :

$$h^E = k(1-k)(\alpha + k\beta), \quad s^E = k(1-k)(\sigma + k\tau) \quad (4)$$

To consider ordering phenomena in the system  $(\text{Hg}_{3-3k}\text{Ga}_{2k}\text{V}_k)\text{Se}_3$  containing structural vacancies  $\text{V}$ , we introduce Gaussian ordering terms of the following type [1]

$$g_{k^*}^s(T, k) = -\Delta_{\text{Tr}} G_{k^*}^0 \exp\left[\frac{(k - k^*)^2}{2\sigma_{k^*}^2}\right] \quad (5)$$

with

$$\begin{aligned} \Delta_{\text{Tr}} G_{k^*}^0 &= \Delta_{\text{Tr}} H_{k^*}^0 - T \Delta_{\text{Tr}} S_{k^*}^0 \quad \text{for } T < T_{\text{Tr},k^*} \text{ and} \\ \Delta_{\text{Tr}} G_{k^*}^0 &= 0 \quad \text{for } T \geq T_{\text{Tr},k^*}. \end{aligned}$$

$\Delta_{\text{Tr}} G_{k^*}^0$  describes the difference between the Gibbs energy of the totally disordered state and the ordered state of the superstructure with the exact stoichiometry  $k^*$ .  $\Delta_{\text{Tr}} H_{k^*}^0$ , and  $\Delta_{\text{Tr}} S_{k^*}^0$  are the molar enthalpy and entropy for the transition from the fully ordered state to the totally disordered state of the pure stoichiometric compound. The exponential expression with its characteristic term  $\sigma_k$  determines, how fast the ordering contribution decreases with increasing distance  $k - k^*$  from the exact stoichiometric composition.

The mean molar Gibbs energy according to Eq. (3) yields for the whole sub-solidus region a single continuous function showing relative or absolute minima near the mole fractions  $k^*$  of the super structures (Fig. 5).

Miscibility gaps occur in all regions in which the  $g$ -function shows a negative curvature. To determine the boundaries of a miscibility gap, one has to calculate the compositions  $k'$  and  $k''$  for which on both sides of the gap the chemical potentials for each component are equal, i.e.  $\mu'_i = \mu''_i$  with  $i \in \{\text{Hg}_3\text{Se}_3, \text{Ga}_2\text{VSe}_3\}$

$$\mu_{\text{Hg}_3\text{Se}_3}^{*\Phi}(k) = g^{*\Phi}(k) - \left(\frac{dg^{*\Phi}}{dk}\right)k \quad (6)$$

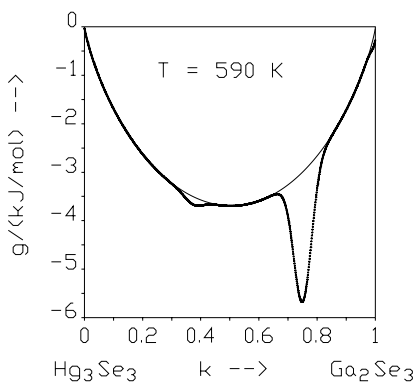


Fig. 5. The mean molar Gibbs energy  $g$  as function of the  $\text{Ga}_2\text{Se}_3$  mole fraction  $k$  for  $T = 590$  K. The inner thin line does not consider the influence of the ordering parameters  $\sum g_{k^*}^s$  of Eq. (3).

$$\mu_{\text{Ga}_2\text{VSe}_3}^{*\Phi}(k) = g^{*\Phi}(k) + \left(\frac{dg^{*\Phi}}{dk}\right)(1-k) \quad (7)$$

Such miscibility gaps behave in the same way as spinodal miscibility gaps. The index (\*) indicates that the so-called normalized  $g$ -functions [13] were used. For the liquid phase this normalized function reads [2]:

$$g_{\text{liq}}^* = \sum_i x_i \left[ RT \ln x_i + \Delta_{\text{F}} H^0(i) T \left( \frac{1}{T} - \frac{1}{T_{\text{F}}(i)} \right) \right] + g_{\text{liq}}^{E,n} \quad (8)$$

Equilibria between the liquid and the solid phase are characterized by the points of contact of the common tangents on  $g_{\text{liq}}^*$  and  $g_{\text{sol}}^*$ .

### 3.2. The ordering parameters

Although we observed the homogeneous ‘3/8-phase’ of the tetragonally ordered ‘t1’-structure at  $k = 0.35$ , we assume that the ideal stoichiometric composition for the fully ordered structure is  $k^* = 0.375$ . We do so, because the X-ray pattern of the observed tetragonal structure corresponds very well with the patterns of the ‘3/8-structures’ of other II–VI/III–VI-systems and because the fully ordered form of this type of structure, composed of only two different clusters  $(\text{HgHgHgGa})\text{Se}$  and  $(\text{HgHgGaV})\text{Se}$ , demands a composition corresponding to  $k = 0.375$ . As to the ordering parameters of the super structures (Table 5) we started the calculations by estimating values for the transition temperature and the transition entropy of the order–disorder processes. The transition enthalpies for disordering are then obtained by the well known equilibrium relation  $\Delta_{\text{Tr}} H^0 = T_{\text{Tr}} \Delta_{\text{Tr}} S^0$ .

### 3.3. Transition temperatures

DTA experiments yield for the ordered structure (t1) near  $k^* = 0.375$  a transition temperature of  $T \approx 630$  K.

As the chalcopyrite phase ( $k^* = 0.75$ ) melts before disordering, a starting value for the determination of its transition temperature was estimated by extrapolation of the border lines of the miscibility gap.

The transition temperature of  $T = 1003$  K for the monoclinic phase at  $k^* = 1$  was taken from the literature [12].

Table 5  
Ordering parameters for  $(\text{Hg}_{3(1-k)}\text{V}_k\text{Ga}_{2k})\text{Se}_3$

Symmetry	$k^*$	$\Delta_{\text{Tr}} H_{k^*}^0$ J/mol	$\Delta_{\text{Tr}} S_{k^*}^0$ J/(mol K)	$T_{\text{Tr},k^*}$ (K)	$\sigma_k$
t1	0.375	2460	3.90	631	0.03
t2	0.75	5000	3.94	1269	0.03
mo <sup>a</sup>	1.0	600	0.60	1003	0.012

<sup>a</sup> Reference [12].

### 3.4. Transition entropies

As derived in [1] the ideal molar mixing entropy for solid solutions of type  $(\text{Hg}_{3-3k}\text{Ga}_{2k}\text{V}_k)\text{Se}_3$  is given by:

$$s_{\text{M}}^{\text{id}}(k) = -R[k \ln k + (1 - k)\ln(1 - k)] \quad (9)$$

If a totally ordered superstructure transformed into an ideally mixed solid solution its order–disorder transformation entropy could be identified with the mixing entropy according to Eq. (9) ( $s_{\text{M}}^{\text{id}}(0.375) = 4.675 \text{ J}/(\text{mol K})$ ,  $s_{\text{M}}^{\text{id}}(0.75) = 5.500 \text{ J}/(\text{mol K})$ ). But, from several II–VI/III–VI systems we know, that a solid solution in equilibrium with its superstructure at the transition temperature is partially ordered. The reason is that also in the solid solutions the clusters forming the ordered structures- here  $(\text{HgHgHgGa})\text{Se}$  and  $(\text{HgHgGaV})\text{Se}$  at  $k = 3/8$ , and  $(\text{HgGaGaV})\text{Se}$  at  $k = 3/4$ -occur with higher than statistical probabilities. Thus, the real disordering entropies must be lower than the ideal limiting values according to Eq. (9). Moreover, we know from the  $c/a$ -ratios (Table 2) that in contrast to the telluride  $\text{HgGa}_2\text{VTe}_4$  the corresponding selenide  $\text{HgGa}_2\text{VSe}_4$  is nearly totally ordered. Thus, it is to be expected that the transition entropy for the chalcopyrite phase in the selenide lattice is distinctly higher than in the telluride lattice.

As starting values for the determination of the disordering entropies at  $k^* = 0.375$  and  $k^* = 0.75$  we used the values that were determined for the equivalently ordered phases in the telluride system  $(\text{Hg}_{3-3k}\text{Ga}_{2k}\text{V}_k)\text{Te}_3$  [14]. Compared to the telluride system, the finally adjusted values for the selenide system (Table 5) are for both tetragonal structures, t1 and t2, nearer to the ideal limiting values.

The disordering entropy of pure  $\text{Ga}_2\text{VSe}_3$  ( $k = 1$ ) was determined in [11] as  $\Delta_{\text{Tr}}S^0 = 0.6 \text{ J}/(\text{mol K})$ . This rather small value suggests a small difference in the degree of order between the solid solution and the ordered structure.

Obviously, the  $\text{Ga}_2\text{VSe}_4$ -rich solid solution is far from being randomly disordered, i.e. the probabilities of the clusters  $(\text{GaGaVV})\text{Se}$  and  $(\text{GaGaGaV})\text{Se}$  forming the ordered structure must be distinctly higher, and those of the remaining clusters  $(\text{GaGaGaGa})\text{Se}$ ,  $(\text{GaVVV})\text{Se}$  and  $(\text{VVVV})\text{Se}$  distinctly lower than in a purely statistical cluster distribution. Such a similarity of solid solution and ordered structure also explains, why the ordering enthalpy is so small, and why no DTA signal could be measured near the order–disorder transition temperature of  $T = 1003 \text{ K}$ . As above mentioned, the totally ordered structure can only be attained after long annealing processes and it gets destroyed by alloying very small amounts of  $\text{HgSe}$ .

### 3.5. The interaction parameters and the fusion data

The fusion data (Table 6) are known from the literature. Initial values for the interaction parameters are determined by adjusting the calculated liquidus and solidus lines to the experimental DTA data. Then, the interaction parameters (Table 7) and the ordering parameters (Table 5) were deter-

Table 6

Fusion data

Substance $i$	$\Delta_{\text{F}}H^0(i)$ (kJ/mol)	$T_{\text{F}}(i)$ (K)	$\Delta_{\text{F}}S^0(i)$ (J/(mol K))
$\text{Hg}_3\text{Se}_3$	93.0 <sup>a</sup>	1072 <sup>b</sup>	86.8
$\text{Ga}_2\text{Se}_3$	20.0 <sup>c</sup>	1283 <sup>d</sup>	15.6

<sup>a</sup> Reference [15].

<sup>b</sup> Reference [16].

<sup>c</sup> Reference [11].

<sup>d</sup> Reference [12].

Table 7

Interaction parameters for liquid and solid phases in the system  $\text{Hg}_3\text{Se}_3/\text{Ga}_2\text{Se}_3$ 

Phase $\Phi$	$\alpha^{\Phi}$ (J/mol)	$\sigma^{\Phi}$ (J/(mol K))	$\beta^{\Phi}$ (J/mol)	$\tau^{\Phi}$ (J/(mol K))
Liquid	–12000	0.0	8000	0.0
Solid	1060	3.5	360	1.2

mined by fitting the calculated boundaries of the miscibility gaps to the experimental data.

The lines drawn in Fig. 1 represent the boundaries of the stable regions in the phase diagram calculated from the Gibbs energy function by use of the adjusted parameters as given in Tables 5–7. The calculated characteristic points of the phase diagram are listed in Table 8.

## 4. The thermodynamic factor

Using the total excess Gibbs energy,  $g^{\text{E}} = g^{\text{E,n}} + \sum g_{k^*}^{\text{s}}$  according to Eq. (3), the thermodynamic factor  $F$  for systems with ordering tendencies can be calculated by the usual expression:

$$F(k, T) = 1 + \frac{k(1 - k)}{RT} \left( \frac{\partial^2 g^{\text{E}}}{\partial x^2} \right) \quad (10)$$

This procedure has the advantage, that the thermodynamic factor for the quasibinary system becomes a single function including all regions of the phase diagram (Fig. 6).

Regions, where  $F < 0$ , are unstable, all others are stable with respect to diffusion [17], but these stable regions can have different characteristics: if  $0 \leq F \leq 1$  is fulfilled, they belong to disordered solid solutions, but they generally extend into miscibility gaps forming thermally metastable regions. Regions with  $F > 1$ , however, belong to stable ordered phases.

Table 8

Calculated characteristic points

Equilibrium (A–B–C)	$T$ (K)	$k$ (A)	$k$ (B)	$k$ (C)
(c1–t1–t2)	610	0.29	0.35	0.75
(t2–c3–mo)	772	0.76	0.97	0.99
(cl–liq–c2)	1064	0.21	0.21	0.21
(liq–c2–t2)	1080	0.44	0.56	0.74
(liq–t2–c3)	1147	0.70	0.77	0.87

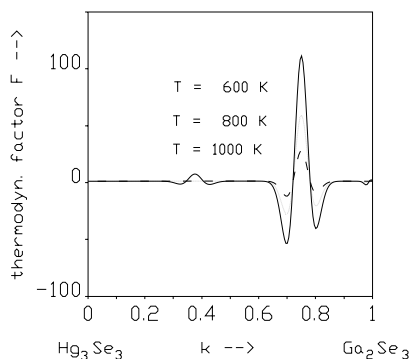


Fig. 6. The thermodynamic factor as function of the  $\text{Ga}_2\text{Se}_3$  mole fraction  $k$  for  $T = 600, 800$  and  $1000$  K; the higher the temperature, the lower the extrema of the thermodynamic factor caused by ordering.

In ordered regions on the one side diffusion would be enhanced by the thermodynamic factor, but on the other side the diffusion should be decreased because the structural vacancies in an ordered region do behave no more as defects but as interstitial sites of the super structure. Thus, for ordered regions of II–VI/III–VI systems one cannot predict, whether the diffusion coefficient will increase or decrease related to the surrounding disordered regions.

## References

- [1] V. Leute, *Calphad* 20 (1996) 407–418.
- [2] V. Leute, H. Bolwin, *Solid State Ionics* 141–142 (2001) 279–287.
- [3] L. Prigogine, R. Defay, *Chemische Thermodynamik*, VEB Deutscher Verlag für Grandstoffindustrie, Leipzig, 1962, p. 244.
- [4] V. Leute, H. Plate, *Ber. Bunsenges. Phys. Chem.* 93 (1989) 757–763.
- [5] D. Lübbers, V. Leute, *J. Solid State Chem.* 43 (1982) 339–345.
- [6] V. Leute, *Ber. Bunsenges. Phys. Chem.* 96 (1991) 713–720.
- [7] V. Leute, H.M. Schmidtke, *J. Phys. Chem. Solid* 49 (1988) 1317–1327.
- [8] A. Zeppenfeld, V. Leute, *Ber. Bunsenges. Phys. Chem.* 96 (1992) 1558–1564.
- [9] V. Leute, H.M. Schmidtke, *J. Phys. Chem. Solids* 49 (1988) 409–420.
- [10] L. Gastaldi, M.G. Simeone, S. Viticoli, *Solid State Commun.* 55 (1985) 605–607.
- [11] M. Kerkhoff, V. Leute, *J. Alloys Comp.* 381 (2004) 124–129.
- [12] R. Ollitrault-Pichet, J. Rivet, J. Flhaut, *J. Solid State Chem.* 33 (1980) 49.
- [13] V. Leute, H.-J. Köller, *Z. Physikal. Chemie NF* 149 (1986) 213–227.
- [14] V. Leute, D. Weitze, A. Zeppenfeld, *J. Alloys Comp.* 289 (1999) 233–243.
- [15] J. Steininger, *J. Appl. Phys.* 41 (1970) 2713.
- [16] Th.B. Reed, *Free Energy of Formation of Binary Compounds*, MIT Press, Cambridge, MA, 1971.
- [17] A.R. Allnatt, A.B. Lidiard, *Atomic Transport in Solids*, Cambridge University Press, 1993, p. 145.